

Software Development, Unit Testing, and the ModelE Climate Model

Nicholas Esposito

February 9, 2015

Department of Atmospheric and Oceanic Science

University of Maryland

College Park, MD

Research Advisor: Dr. Anil Deane

Academic Advisor: Dr. Sumant Nigam

ACKNOWLEDGEMENTS

I would like to thank Dr. Anil Deane for the opportunities and advice he has given throughout my time at the University of Maryland. The guidance, encouragement and advice given in my work and throughout the creation of my scholarly paper are greatly valued, and the knowledge gained will continue to stick with me as I continue with my post-graduate career. Additionally, I would like to thank my academic advisor, Dr. Sumant Nigam, for his invaluable guidance throughout my career as a Graduate Student at the University of Maryland. I would also like to thank the Department of Atmospheric and Oceanic Science here at the University of Maryland for leaving me with the essential skills and knowledge that are essential to be a productive and esteemed member of society. Finally, I would like to thank my parents, family, and friends, for their limitless guidance, praise, and support throughout my years as a student.

Contents

1	Abstract	4
2	Background	5
2.1	Software Development	5
2.2	Agile Development and Test Driven Development	6
2.3	Unit Testing	7
2.4	Testing Framework: pFUnit	7
2.5	Verification and Validation	8
3	Shallow Water Equation Model	9
3.1	Physical Results of the Shallow Water Equation Model	10
3.2	pFUnit Test Results	11
4	GISS ModelE	13
4.1	Overall Model Structure	13
4.1.1	The Atmospheric Model	14
4.1.2	The Ocean/Ice Model	16
4.1.3	The Land Surface Model	18
4.1.4	Tracers	18
4.2	Validation of ModelE	19
4.2.1	Sea Level Pressure	20
4.2.2	Surface Wind Speed and Direction	21
4.2.3	Zonal Wind	22

4.2.4	Atmospheric Temperature	23
4.2.5	Sea Surface Temperature	24
4.2.6	Precipitation Patterns	25
4.2.7	Conclusions from the Validation	26
5	Conclusions and Future Work	27
6	References	28
7	Tables	31
7.1	Table 1: Calculated SWE Model Errors	31
7.2	Table 2: Calculated SWE Model Errors for edited code	31
8	List of Figures	32
8.1	Original Rossby Soliton Solution	32
8.2	Edited Rossby Soliton Solution	33
8.3	Sea Level Pressure	34
8.4	Surface Wind Speed and Direction	35
8.5	Zonal Wind	36
8.6	Atmospheric Temperature	37
8.7	Sea Surface Temperature	38
8.8	Precipitation Patterns	39

1 Abstract

The principles of software development and engineering dictate how creating or updating software should be handled. Unit Tests will be used on the a Shallow Water Equation Model, and the NASA GISS ModelE climate model in order to make continuing development more efficient and accurate throughout the development process. In order to do this, small, efficient, and easily understandable tests will be created for each part of the source code. This code development will incorporate the test, as opposed to most testing, which occurs after a code is written. Agile and Test-Driven Development Techniques, which are subdisciplines of software development, will be used in order to make this process quick and efficient, and will be explained in detail. Validation of the model shall also be performed on the existing model to determine climate simulation capabilities. The final goal of this project will be a methodology and tools to be used for better unit testing and code development.

2 Background

2.1 Software Development

The practice of software development is defined as a set of activities that results in software products. Software development may include new development, modification, reuse, re-engineering, maintenance, or any other activities that result in software products (Npd-solutions.com, 2007). There are many alternatives involved in software development, and each must be carefully executed in order to produce the best product possible.

There is a certain methodology that should be followed when entering a cycle of software development. First is the planning stage. Here, all of the requirements should be understood, including the computational environment to develop the software, and other programs that may have to be used in order to get the program working.

Next is the designing phase, where the steps to create the software are written. Next is the implementation, where the actual code is written. The next step includes both testing and documentation. This ensures there are no bugs or errors, and makes a log of everything included with the software. The second to last step is deployment of software. Here, all of the code written is placed together in a logical fashion. The final, ongoing step is the maintenance of the software. The product needs to be as complete as possible at this point.

2.2 Agile Development and Test Driven Development

Agile Development and its techniques provide instructions for how to successfully and efficiently create and test software. The Scrum Handbook suggests it is a framework within which people can address complex adaptive problems, while productively and creatively delivering products of the highest possible value (Sutherland & Schwaber, 2013).

Agile development splits each coding job into small increments. These iterations are performed on short time frames of five days to up to four weeks. This short time frame reduces risk and allows the project change if need be. Due to the short time frames, it is expected that each iteration may be released. These short time frames allow agile development to be an adaptive method. This means adapting quickly is important, as instructions may change in an instant. There tends to be no set future goals, and things happen on a day-to-day or week-to-week basis.

There is actually a process for creating each and every test. Beck (2002) explains all of the following in his book on Test-Driven Development. There are 5 main steps that are essential to test making.

The first is to add a little test. Second, run all tests and see the new one fail. This increases our confidence that we are testing the right thing. Third, make a little change to cause the test to pass. Fourth is to run the tests see them all succeed. If it doesn't pass, return to step 3 and redo until the test passes. The final step is to refactor the code to remove duplication.

2.3 Unit Testing

Unit testing is a method of software development using modules that create code in order to pass a test (Beck, 2002). Most test cases tend to be independent from others, while testing different parts of codes to make sure each works. Unit tests are primarily done earlier on in development, in order to ensure the basic functions of the program are correct.

There are certain unit testing techniques that need to be noted. The tests should be effective. There needs to be a focus on the performance of the components of the code, and write the test in the smallest amount of code possible. Write a clean environment for each test and write each test from scratch. The use of mock objects is also highly encouraged.

2.4 Testing Framework: pFUnit

Many codes need to be tested in a certain environment, and they are called testing frameworks. The framework used in this project is called pFUnit. It is primarily used in the Java or Fortran programming language and usually within Eclipse. In this case, it was used to test ModelE code, which is written in Fortran. pFUnit was actually created with ModelE in mind, so it's very clear that the environment of pFUnit is fully capable of handling the ModelE software (Rilee, 2014). The shallow water equation model was unit tested in the pFUnit environment.

2.5 Verification and Validation

Presented above is an understanding of the theory and process of software development, and all of the steps that must be taken into account when producing software. A Shallow Water Equation Model was selected as being of intermediate complexity to the full climate capability of ModelE. The NASA GISS ModelE climate model was selected as a GCM, because it is an open-source model that is consistently being updated. First and foremost, the model needed to be evaluated on how it performs. This can be done through verification and validation of this software.

Validation is the evaluation of software during or at the end of the development process to determine whether it satisfies specified requirements (IEEE, 2011). In essence, this is to be sure that the program created actually meets a user's needs, and is useable. Verification is evaluating software to determine whether the products of a given development phase satisfy the conditions imposed at the start of that phase(IEEE, 2011). In essence, it makes sure code is built it correctly, and meets all demanded specifications.

Both must be taken into account when creating a project, kept in mind while working on it, and then evaluated at the end of the project. The most recent work for this project has been validating ModelE climate outputs in order to familiarize oneself with the quality of the climate simulations.

3 Shallow Water Equation Model

Before the jump from testing simple codes to large-scale modeling, it was necessary to make an intermediate step in atmospheric modeling. This was done with the help of a shallow water equation (SWE) model developed by Dr. Iskandarani at the University of Miami.

As a brief review, the shallow water equations are used to describe atmospheric flow, where the horizontal length scale (such as waves) is much greater than the vertical length scale (in this case, the height of the atmosphere). It is derived using the Navier-Stokes equations, which describe fluid motions. These equations themselves are derived using the laws of conservation of mass and momentum.

The model is significantly simpler than modelE, which is a large-scale climate model. The SWE model simply deals with waves, with only forces of gravity and Coriolis. The model is centered at the equator, such that Coriolis force is near 0, but still has some small impacts on motions and waves with increasing distance north or south of it. It doesn't take into account topography at the surface and also does not make a distinction of where on the equator this is centered.

It is noted that the SWE model is used for general calculations and studies of how atmospheric motions should work in an ideal setting. Most variables have preset values. For example, both depth of the fluid and gravitational acceleration are simply unity in their respective nondimensional units. The strength of the Coriolis force increases linearly with distance from the equator and does not vary with latitude. These may be changed by simply changing the inputs for the model, which are listed in the file `shallow.in`.

Resolutions for the model are among the variables that may be changed, though $.5^\circ$, $.25^\circ$, or $.125^\circ$ are the most commonly used. The default time-step is .02 seconds for the coarsest resolutions. The default number of time-steps is 2000, though this may be changed to however many time-steps are desired (Iskandarani, 2013).

The model discretizes the shallow water equations using the finite differencing method, with the variables being staggered across an Arakawa C-grid. The code's default initial conditions simulate the propagation of an equatorial Rossby soliton. Its dynamics are dependent on the changing of wave amplitude that arise from the Coriolis terms and non-linear terms in the equations. The code initializes the Rossby soliton as a solution with asymptotes. The domain of the model is centered on a Beta-plane centered at the equator. The default x-dimension is three times the y-dimension, and the Coriolis terms is dependent on the distance from the equator. It's strength may be altered using the subroutines given with the model (Iskandarani, 2013).

Running the model with all conditions described generates three separate files, for zonal velocity, meridional velocity, and the pressure at each grid point. These may then be plotted, showing the Rossby soliton solution (Figure 1). Additionally, the model calculates RMS error and maximum error, both of which are important to determining whether or not the model's outputs are valid.

3.1 Physical Results of the Shallow Water Equation Model

After the SWE model's mechanics were understood, unit testing was next. In order to do this, we used all of the preset conditions for the model and simply let

the code run with the default initial conditions. The Rossby soliton solution (Figure 1) is what is described as our “original.” Theoretically, if we were to change any of the original code, then the model would compute a new solution, which would be compared to the initial soliton solution. Figure 2 is the Rossby soliton solution when we take the code and alter the file `shrhs.f90` such that the value of zonal wind is altered. The model was run again with this newer value, so the a ‘new’ Rossby soliton was produced that was different from the ‘original’ solution. When comparing Figure 1a and 2a, the difference is most apparent at the left and right edges.

As mentioned, the Rossby solitons solutions are produced as three separate files of zonal speed, meridional speed, and pressure at each grid point. We were able to evaluate the value at each grid point for both solutions and for all variables. The unit test then compared these two values, first by subtracting the value of u , v and z_t at each grid point, defined as the “error”. Each grid point’s error was used in the calculation of the Root-Mean-Squared (RMS). To calculate RMS, each value for “error” was squared and summed up. That value was then divided by the number of grid points. Finally, the square root of that value was taken as the RMS.

3.2 pFUnit Test Results

Within pFUnit, three tests were created, one for each variable. For the three variables, the maximum and minimum values, the maximum error, and Root-Mean-Squared (RMS) were computed. The test compares the grid point values for each property. The values would be considered equal if they were within an arbitrarily small “tolerance” value, and also if they were within the maximum and RMS error.

The value chosen is user-dependent and may be increased or decreased depending on how accurate a user thinks it should be. The ‘original model’ error values proved to be very small and are shown in Table 1. The altered or ‘new’ solution errors are plotted in Table 2. Notice that the zonal wind errors are drastically different, while the the others have remained the same. Therefore, these can be factored into our unit test, which can then be used to check to see if the Rossby soliton solutions are the same. As previously stated, the solutions are not the same, and the test proves this by failing.

A sample code for an assertion is shown below. This asserts that RMS is no greater than the number preceding it, which is the tolerance. If the RMS is greater than this number, then the test fails. A similar test code was written for the maximum difference between Rossby soliton solutions.

```
@assertGreaterThanOrEqual(2.886157E-017,RMS)
```

When the test was run with the two different Rossby soliton solutions, the test ending up failing (shown below), indicating that the solutions were sufficiently different such that they can no longer be considered the same. Of course, this is still dependent on the tolerance that is chosen. If a larger tolerance is chosen, then the new solution can be much more different than the original without failing the test. Therefore, these tests may have to be edited on a case by case basis for other models.

```
expected +0.2886157E-18 to be greater than or equal to: +0.2886057E-17.
```

```
FAILURES!!!
```

```
Tests run: 3, Failures: 1, Errors: 0
```

The direct result of unit testing the SWE is that there is now a framework for how to handle the modeling the NASA GISS ModelE. The techniques used above would also be applied to the ModelE results, in order to ensure that any changes to the model code do not produce noteworthy differences between the model outputs.

4 GISS ModelE

ModelE is a General Circulation Model (GCM) developed by NASA GISS, and has been in continuous use for at least 25 years. This current version is a rewrite of previous models, but this particular model has been through myriad advancements over the years. There are many components of this model, including the standard atmosphere, open water and oceans, sea ice, glaciers and even land surface variables such as soil moisture content. The newer version has updates of the physics, stratospheric circulation and forcing fields of the model. New additions include tracers of heat, humidity, atmospheric chemistry, aerosols and even the carbon cycle.

4.1 Overall Model Structure

The model has a resolution typically seen with other GCMs. Horizontally, the resolution can be $4^\circ \times 5^\circ$, or as small as $2^\circ \times 2.5^\circ$. These higher resolutions are performed to limit the length and variability of the experiments. Vertically, the model can be run with 20 or 23 layers, depending on the highest pressure level that needs to be studied. The 20-layer reaches up to .1 hPa, while the 23-layer reaches to .002 hPa. This is done to better resolve motions in the stratosphere and mesosphere.

Initialization of the model is handled by a subroutine called `INPUT`, which initializes all variables of the model. An initial date must be chosen so that the model knows the values to input. These are all handled by multiple subroutines that are responsible for each grouping of variables. For example, the atmospheric and ocean variables are handled by different subroutines, even though they may be dependent on one another, but this is not needed for the initialization.

After the initialization, the main program runs with the help of the `MAIN` Program. There is a 15-step calling order that `MAIN` uses that cannot be changed. It starts out with large atmospheric features, such as atmospheric dynamics, atmospheric water phase changes, and radiative transfer calculations. Next, it calculates water fluxes into and out of oceans via rivers and evaporation, and ice fluxes. At the end, a number of subroutines calculate changes compared to the climatology (Rind et al, 1988).

Every diagnostic that is run within the model is summed up at the end of each month. ModelE obtains results for each month, instead of each individual day. These values may be averaged during post-processing by dividing each month by the number of days in each month, which computes average daily values over each month. Once post-processing is completed, it is possible to average these diagnostics over any time period within a test run.

4.1.1 The Atmospheric Model

The atmospheric model component of ModelE is the most detailed. ModelE uses a leap-frog time stepping time s_{rep} every 8 leap-frog steps. This is done to prevent

solution splitting, and helps in conserving energy in the atmosphere.

Most of the atmospheric dynamics of the model are based on dry-air physics. This is done so that there would be no effect of water vapor on mean sea level pressure. Instead, water vapor is factored into potential temperature. Water vapor is still plotted as a tracer. Cloud processes are based on convective towers that form with upward vertical motion of the model, are equipped to handle fluxes of water vapor and heat into or out of a cloud. Moist-air physics only take place during large-scale moist convection (thunderstorms) and other large scale convection systems (mesoscale convective complexes and hurricanes) (Yao and Del Genio, 1996). A subroutine that handles moist convection is also based on convective towers. The most important part of this subroutine is entrainment of dry air outside each plume, which can affect cloud-top height and radiative fluxes. Radiative fluxes themselves are calculated over 33 spectral intervals in the visible solar and long-wave infrared wavelengths (Oinas et al, 2001).

Planetary boundary physics take effect when calculating surface fluxes between each land surface type. These types are open water, earth and soils, and land ice. Calculations at very high resolutions take place up to 10 meters above ground level that determine this small layer's atmospheric characteristics.

A turbulence scheme is used when determining which diffusion parameters to use. Since motions and turbulences tend to accelerate very quickly in the planetary boundary layer, these calculations are completed multiple times per hour. Outside of this 10-meter layer, vertical mixing in the model occurs if two adjacent grid boxes are statically unstable, and is also dependent on the amount of turbulent kinetic

energy available.

Due to the importance of stratospheric motion on tropospheric characteristics, such as jet stream height and tropopause temperature, it must also be resolved. Gravity waves and stratospheric drag are among the most important aspects of the model in this respect. The stratospheric drag formulation is applied as Rayleigh damping near the top of the model, such that predetermined values evaluate the rate at which frequencies of motions will damp. These values are dependent on upper-atmospheric disturbances, such as large-scale, deep convection, and gravity waves (Rind et al, 1988).

4.1.2 The Ocean/Ice Model

The ocean component of the model is a very dynamic one, with many different parts. The most basic ocean model that uses a monthly varying quantities, such as Sea Surface Temperature (SST), Sea Surface Salinity (SSS), and sea ice, that are based on the result of previous simulations. The monthly outputs are used to calculate and interpolate a fixed daily value at each grid point. This is done in a way such that the average of all of the daily values at each grid point is equivalent to its mean monthly value.

A mixed-layer model is used in order to calculate heat and freshwater fluxes into or out of the ice and ocean components of the model. The climatology of the depth of the mixed layer depth, along with measured ocean heat fluxes, are combined to determine the ocean heat flux outputs. Due to the high impact of ice advection on ocean heat fluxes especially in the northern hemisphere, a large part of the model

is devoted to calculating it. It may be necessary to turn off this parts of ModelE, because it may take decades for thermal equilibrium to take place in the model when radiative forcings are applied.

As for the dynamics of the ocean, the Boussinesq approximation is not assumed, so density is dependent on motions (Russell et al, 1995), allowing the model to more easily calculate physics that require the conservation of mass. A number of schemes are applied to mixing of quantities, such as momentum and eddy flux. One of the main issues of water transport was the sub-grid nature of numerous water flows, such as the small straits that mix different larger bodies of water. Fluxes into and out of the water bodies connected by the straits are treated as functions of the pressure gradients in either direction. Due to the large differences in these pressure gradients in the vertical and sometimes horizontal direction, there is a drag coefficient that acts to moderate the fluxes. (Visbeck et al, 1997)

The Ice component of the model is somewhat different and has two main layers. The first layer is 0.1 meter thick ice that may have any amount of snow on top of it, and the second is at least .1 meter thick ice that can grow to any thickness. Each layer contains measured characteristics, such as temperature and heat, but even some tracers like sea salt or green house gas concentrations. Ice accretion and melting are measured constantly because they may impact the larger ocean-atmosphere system, especially during heat release and melting (Rind, et al, 1988). These are also important to take a note of because Earth albedo is known to be very important in determining radiative balance.

4.1.3 The Land Surface Model

The land surface component of the model also has multiple components to it. There are only two types of soils: bare and vegetated. If there is determined to be vegetation, an extra canopy layer is added on top of the surface. Both types of soils are modeled using six layers of variable depth. At the surface layer, evapotranspiration and runoff are among the main variables calculated (Hansen 2000).

Large bodies of water that are not directly connected to oceans, such as lakes, are not modeled using ocean dynamics and are instead evaluated within the land surface model. Lake models contain a surface layer down to one meter, and an infinitely large lower layer. Lake size and mass are highly dependent on fluxes into or out of it, and especially by evapotranspiration, rivers, and tributaries. Rivers and tributaries operate on very sub-grid scales, and have very little interaction with the atmosphere. River movement and water fluxes have are more affected by the topography of the grid. This is important because eventually this moving water reaches oceans, where it is spread uniformly throughout the grid point that it reaches the ocean (Schmidt 2004).

4.1.4 Tracers

The tracer model follows all transports of mass and momentum in the model. Most of the tracers are insoluble gases, aerosols, water isotopes, atmospheric chemistry, and air mass qualities. The most important aspect of the tracer model is that it follows mass units, not concentration. Conservation of mass is therefore upheld. Most of the tracers use similar physics schemes, though some tracers require special

physics, some atmospheric chemical reactions for example (Schmidt 2004).

Tracer transport resolution is greater than the horizontal and vertical resolutions. This was done because a better resolution was needed in order to better quantify and follow tracer impacts. These resolutions can be as small as $.7^\circ \times .8^\circ$. It should be noted that tracers are not immediately tracked by the model and need to be turned on via a subroutine.

4.2 Validation of ModelE

In order to determine if ModelE is adequate for climate modeling, it was essential that a validation be performed on the model. The model has previously been validated before, and can be summarized in numerous papers, notably Hansen et al (1998) and Hansen et al (2000). In order to perform our own validation, the model was run for 30 years under what can be considered normal atmospheric and oceanic conditions. The model began December 1, 1950, but it was important to “spin-up” the model, which we gave a year to do. The spin-up allows the atmospheric and oceanic inputs to begin circulating around the globe. The outputs are ready to be evaluated after this one year spin-up. The resolution chosen was $2^\circ \times 2.5^\circ$ horizontally and 20-level vertically. Again, data is aggregated at the end of each month, and post-processing of the data allowed evaluation of the average daily values for each month.

The 30-year period chosen began on December 1, 1951 and ended on November 30, 1980. The reason the dates were chosen has much to do with the seasons that were evaluated. The months of December, January, and February were chosen as

the winter months. March, April, and May were chosen as spring. June, July, and August were chosen as summer. September, October and November were chosen as autumn. Each season was evaluated by averaging the each three month period with each other three month period over the entire 30-year interval. This average was decided to be called the climatology of each season. The validation was completed by comparing certain outputs of the model to the re-analysis data put out by NCAR. Most of it was summarized in Holton (2004).

4.2.1 Sea Level Pressure

Figure 3 depicts the progression of average sea level pressure throughout the year at the 3 month intervals discussed. During the Boreal winter, the Aleutian and Icelandic Lows are visible in the Northern Hemisphere. The temperature contrast between the cold continents and warmer ocean causes cyclogenesis off of the eastern coasts of the large continents, above the warm ocean currents that flow northeastward. The Siberian High is the strongest high on the map because here, the lowest temperatures occur. The result is very dense air, which occurs due to the hydrostatic approximation. The North American High and Greenland High are also visible, but are much weaker since temperatures are not normally as cold when compared over the Central Asian Highlands.

In the Southern Hemisphere, there is a ring of lower pressure around Antarctica. This occurs from the temperature difference contrasting the warmer ocean water and very cold continent, producing large areas of cyclogenesis. Meanwhile, high pressure occurs in the eastern part of the ocean basins, which is expected.

During the boreal summer, we see the effect of increased insolation on the Northern Hemisphere. The large high pressure centers that dominated the centers of the continents have depleted. Thermal Lows can now be found in South Asia and the southeastern United States, which will initiate the monsoon season in each area. The Pacific High and Bermuda/Azores High are now much stronger and have moved slightly northward, since they do not have to compete with the temperature-gradient initiated cyclones that dominate the North Atlantic and North Pacific during the winter.

4.2.2 Surface Wind Speed and Direction

Figure 4 depicts the progression of surface wind speed and direction throughout the year. In general, we find the weakest winds over land, where frictional forces take effect. Wind speeds are much stronger over the ocean, where there is less friction occurring.

The direction of the wind generally follows the trade winds. Winds tend to converge at the equator, 60°N and 60°S of the equator, and at the center of low pressure. Winds tend to diverge at 30°N and 30°S of the equator, at the poles, and at high pressure centers. The result of this divergence/convergence is that we see by the model.

Coriolis acceleration causes these winds to turn right in the Northern Hemisphere. The direct result is that in the Northern Hemisphere, winds around low (high) pressure are counterclockwise (clockwise), and toward (away from) the center. In the Southern Hemisphere, Coriolis acceleration is toward the left of motion, so that

winds around a low (high) pressure flow clockwise (counterclockwise).

4.2.3 Zonal Wind

Figure 5 depicts the progression of zonal wind throughout the year, from the surface to 10 hPa. West winds are predominate throughout much of the atmosphere, and peak eastward motion occurs in the jet streams. Slight easterly winds are seen at the equatorial surface and in the stratosphere.

The jet streams shown are produced as a result of the thermal wind relation. The thermal wind relation states that vertical wind shear is dependent on the horizontal temperature gradient. Therefore, a very strong horizontal temperature gradient would produce very large shear, or in this case, a jet stream.

It is shown that the tropospheric jet streams are roughly similar strength during their peak in the winter months. This is not what happens in the actual atmosphere, however. The Northern Hemisphere jet should be slightly stronger, which is due to the larger seasonal contrasts in temperature, as seen above. The Southern Hemisphere, which is dominated by open ocean, does not experience a large seasonal contrast. Another direct result of this is the Southern Hemisphere jet is much more constant year-round (in the vicinity of 35 kts year-round), while the Northern Hemisphere jet tends to change much more in strength (about 17.5 kts during summer compared to greater than 35 kts during winter).

Additionally, the strongest jets should actually occur just below the tropopause, or at 200-300 hPa. ModelE does not show this in the figure, and instead shows jet strength in some seasons actually increasing through the stratosphere. This indicates

that ModelE may not adequately model stratospheric motions.

4.2.4 Atmospheric Temperature

Figure 6 depicts the progression of atmospheric temperature throughout the year, from the surface to 10hPa. The temperature at the surface in the mid-latitudes is highly dependent on which season it is. Due to axial tilt, the Northern Hemisphere experiences much more direct sunlight during the boreal summer months, while the Southern Hemisphere experiences much less direct sunlight. The poles also tend to experience larger temperature changes due to the seasons. In contrast, there is much less temperature variation in the tropics, since the Sun is almost directly above year-round.

The coldest region of the atmosphere is near the tropical tropopause. This is a result of strong solar heating at the surface, and high moisture content producing a very unstable boundary layer. This air is positively buoyant and accelerates upward. The air will cool dry adiabatically at 9.8°C per kilometer until it begins to condense at the Lifting Condensation Level (LCL). The air will continue to cool moist adiabatically as it rises until it reaches the Equilibrium Level (EL), or the Level of Neutral Buoyancy (LNB). Some parcels of air are so unstable that they regularly punch through the tropopause and into the extreme lower levels of the stratosphere. The result of these parcels reaching so high into the atmosphere is that they cool much more than other parcels away from equator, where the surface boundary layer is not quite as warm and unstable. It seems that the model has a very good grasp on tropospheric temperature.

ModelE adequately calculates most stratospheric qualities with the exception of wind speeds. In general, the stratosphere temperature increases with height. This is due to the warming effect of chemical reactions, specifically the breakdown of ozone by uv light into atomic and diatomic oxygen molecules. It is shown that the Southern Hemisphere winter is much colder than the Northern Hemisphere. This is because the Brewer-Dobson Circulation is much weaker in the Southern Hemisphere, which leads to weaker descent in the polar regions and therefore less adiabatic warming.

4.2.5 Sea Surface Temperature

Figure 7 depicts the progression of Sea Surface Temperatures (SST) throughout the year. It seems that the patterns are very well calculated in ModelE. The warmest SST in general occur at the equator, where peak insolation occurs, They also tend to occur in the western boundary currents of the major ocean basins, with the exception of the Arctic Ocean. Peak worldly SST occurs in the West Pacific Ocean, where temperatures are regularly above 27°C. This is roughly the maximum that is expected to occur on Earth, because this warm water allows a large amount of fuel for thunderstorms to form, which block out the Sun and don't allow more radiation to reach the surface.

The Arctic Ocean and the currents that surround Antarctica are the coldest, where insolation is weakest throughout the year. Cooler waters also occur east of the subtropical gyres, where there is equator-ward flow. These are regions of upwelling, which bring cold, nutrient rich water up to the surface, which then cools and stabilizes the atmosphere as well.

There is very weak seasonal variation in SST, as opposed to land-surface atmospheric temperature. This is due to the high heat capacity of water. This indicates that the model does well in regards to chemical and physical properties of oceans and water.

4.2.6 Precipitation Patterns

Figure 8 depicts the progression of precipitation patterns throughout the year. Peak rainfall occurs in a belt around the equator, which is called the Intertropical Convergence Zone (ITCZ). Here, winds at the surface converge and rise. With the help of very warm SST and surface temperatures, air rises, condenses into rain and thunderstorms, which then proceed to produce incredible amounts of precipitation. This continues year-round.

During northern hemisphere winter, it is possible to see storm tracks due to the increase in precipitation that is usually associated with these storms. They are visible east of Japan and somewhat visible east of the United States. Another peak occurs where these storms interact with the land environment and mountains, notably the Rocky Mountain range in the western part of the North American continent. Here, the mountains force moist air parcels upward, which condense, form clouds, and precipitate.

During northern hemisphere summer, these storm tracks disappear as the temperature gradients between land and ocean disappear. The thermal lows created by modelE for the large continents, which are responsible for monsoons in the real world, seem to have initiated very small monsoons, especially over India. It is not

very noticeable in the southwestern US, though that particular monsoon season tends to only last a month or two. Over India, there seems to be a peak of rainfall rates in the southern part of the subcontinent, away from the Himalaya Mountains and the central and northern regions of the country. This likely indicates that the model does not have a good grasp of the monsoons.

4.2.7 Conclusions from the Validation

From these studies, there are clearly some things that modelE is good at recreating, but there also some issues. The model does a good job concerning the atmospheric temperatures and variability, so it likely has a good handle in the thermodynamics of the atmosphere. It also correctly determines trade wind directions, seasonality of high and low pressure zones, and ocean temperatures and dynamics. From this, it can be gathered that the model likely has an acceptable understanding of much of the physical characteristics and dynamics of the atmosphere and ocean.

There are some areas where the model is average, at best. For example, the North American and Indian Monsoon locations are somewhat off or are unable to be seen entirely. Some of this may have to do with geography, which may be due to the resolutions of the model. Resolution may also affect the jet stream strength and variability in the model. ModelE also misses the stratospheric wind profile, which indicates it does not have a good grasp of stratospheric motion, or perhaps even the thermal wind relation, even though it gives the correct temperature profile.

5 Conclusions and Future Work

We have developed a methodology on how to begin unit testing ModelE. There may be some limitations that must be considered when using this model, but we now have at least a general understanding of it. We can use these results of the validation as our control to compare to the newer version of the model once testing has begun.

Current work has been on a shallow water equation model, in an attempt to link simple tests with large-scale coding. Testing on ModelE is the next step, and will be done with pFUnit, on the NASA Discover supercomputer. The “final product” of this project will be an understanding of how to help developers of the ModelE and other, similar codes to develop better codes thanks to the newer techniques involved in unit testing. Theoretically, it will take less time to produce newer codes with the new methodologies. Any and all unit tests written for this project would be shipped with the model code to help developers who wish to edit or add to the code.

6 References

Beck, Kent. *Test-Driven Development: By Example*. Boston: Addison-Wesley Longman 2003.

Del Genio, A. D., M. S. Yao, W. Kovari and K. K. Lo, 1996. A prognostic cloud water parameterization for General Circulation Models. *J. Clim.* 9, 270-304.

Hansen, J., R. Ruedy, A. Lacis, Mki. Sato, L. Nazarenko, N. Tausnev, I. Tegen, and D. Koch, 2000. Climate modeling in the global warming debate. In *General Circulation Model Development* (D. Randall, Ed.), pp. 127-164. Academic Press. San Diego.

Hansen, J. E., Mki. Sato, L. Nazarenko, R. Ruedy, A. Lacis, I. Tegen, T. Hall, D. Shindell, P. Stone, T. Novakov, L. Thomason, R. Wang, Y. Wang, D.J. Jacob, S. Hollandsworth-Frith, L. Bishop, J. Logan, A. Thompson, R. Stolarski, J. Lean, R. Willson, S. Levitus, J. Antonov, N. Rayner, D. Parker and J. Christy 2002. Climate forcings in Goddard Institute for Space Studies SI2000 simulations. *J. Geophys. Res.* 107, 4347, DOI 10.1029/2001JD001143.

Holton, James R. *An Introduction to Dynamic Meteorology*. 4th ed. Amsterdam: Elsevier Academic, 2004. Print.

Hooker, David. "7 Principles of Software Development." Weblog post. N.p., 5 Sept. 1996. Web.

IEEE. "IEEE Guide—Adoption of the Project Management Institute (PMI(R)) Standard A Guide to the Project Management Body of Knowledge (PMBOK(R) Guide)—Fourth Edition." IEEE Xplore. IEEE, 21 Nov. 2011. Web. 25 Oct. 2014. <<http://ieeexplore.ieee.org/xpl/articleDetails.jsp?arnumber=6086685>>

- Iskandarani, Mohamed. "MPO662 Course Material." *MPO662 Course Material*. University of Miami, 2013. Web. 1 Nov. 2014. <[http://rsmas.miami.edu/personal/miskandarani/Course Material](http://rsmas.miami.edu/personal/miskandarani/Course%20Material)>
- "New Product Development Glossary" DRM Associates, 2007. Web. <<http://www.npd-solutions.com/glossary.html>>.
- Rilee, Mike. "PFUnit: PFUnit 3 - Documentation." NASA. 11 Nov. 2014. Web. <<http://pfunit.sourceforge.net/>>.
- Oinas, V., Lacis, A. A., Rind, D., Shindell, D. T., & Hansen, J. E. (2001). Radiative cooling by stratospheric water vapor: Big differences in GCM results. *Geophysical research letters*, 28(14), 2791-2794.
- Rind, D., Suozzo, R., Balachandran, N. K., Lacis, A., & Russell, G. (1988). The GISS global climate-middle atmosphere model. Part I: Model structure and climatology. *Journal of the atmospheric sciences*, 45(3), 329-370.
- Russell, G.L., J. R. Miller, D. H. Rind 1995. A coupled atmosphere-ocean model for transient climate change. *Atmos. Ocean* 33 , 683-730.
- Schmidt, G.A., R. Ruedy, J.E. Hansen, I. Aleinov, N. Bell, M. Bauer, S. Bauer, B. Cairns, V. Canuto, Y. Cheng, A. Del Genio, G. Faluvegi, A.D. Friend, T.M. Hall, Y. Hu, M. Kelley, N.Y. Kiang, D. Koch, A.A. Lacis, J. Lerner, K.K. Lo, R.L. Miller, L. Nazarenko, V. Oinas, J.P. Perlwitz, Ju. Perlwitz, D. Rind, A. Romanou, G.L. Russell, Mki. Sato, D.T. Shindell, P.H. Stone, S. Sun, N. Tausnev, D. Thresher, and M.-S. Yao 2006. Present day atmospheric simulations using GISS ModelE: Comparison to in-situ, satellite and reanalysis data. *J. Climate* 19, 153-192.
- Schmidt, Gavin. "National Aeronautics and Space Administration." *NASA GISS: GISS GCM ModelE: Description and Reference Manual*. N.p., 2004. Web. 17

Dec. 2014. [<http://www.giss.nasa.gov/tools/modelE/modelE.html>].

Sutherland, Jeff, and Ken Schwaber. "The Scrum Guide." Scrum Guide. 2013. Web. 30 Nov. 2014. <<http://www.scrumguides.org/scrum-guide.html>>.

Visbeck, M., Marshall, J., Haine, T., & Spall, M. (1997). Specification of eddy transfer coefficients in coarse-resolution ocean circulation models*. *Journal of Physical Oceanography*, 27(3), 381-402.

7 Tables

7.1 Table 1: Calculated SWE Model Errors

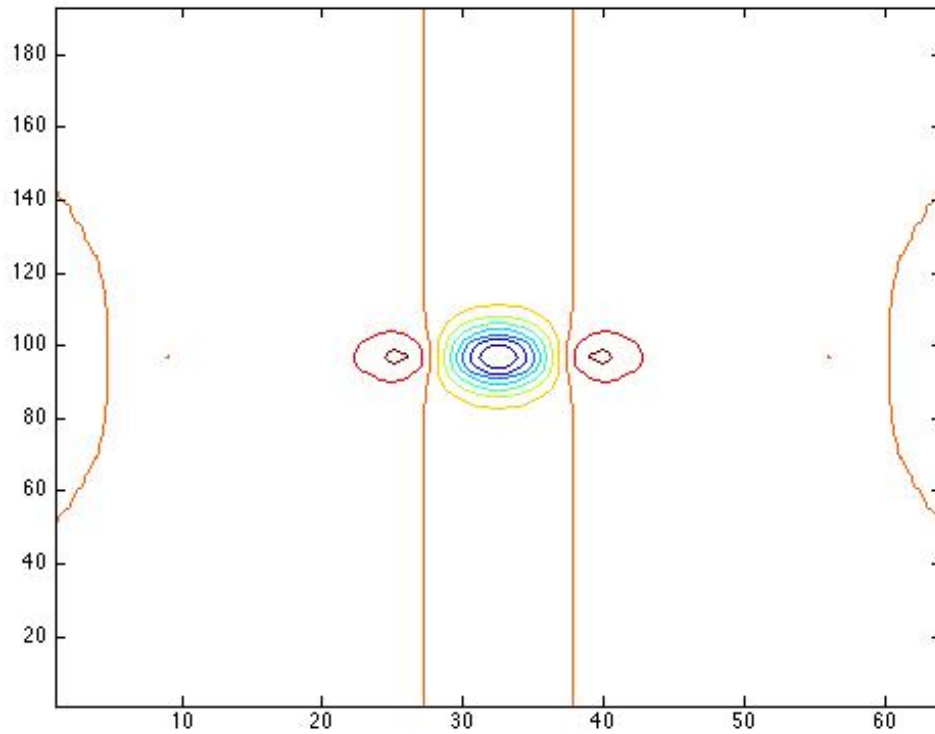
Error type	Zonal Wind	Meridional Wind	Pressure
Max error	0.39114	.092012	.23337
RMS error	0.26365	.093783	.23487

7.2 Table 2: Calculated SWE Model Errors for edited code

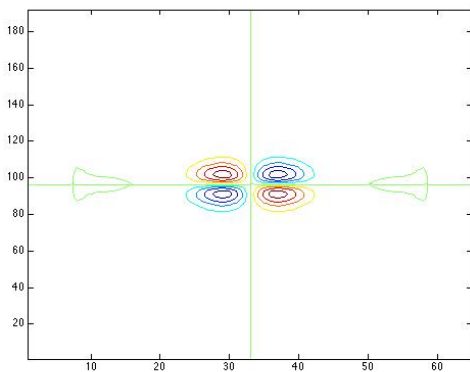
Error type	Zonal Wind	Meridional Wind	Pressure
Max error	120.39	.092012	.23337
RMS error	833.55	.093783	.23487

8 List of Figures

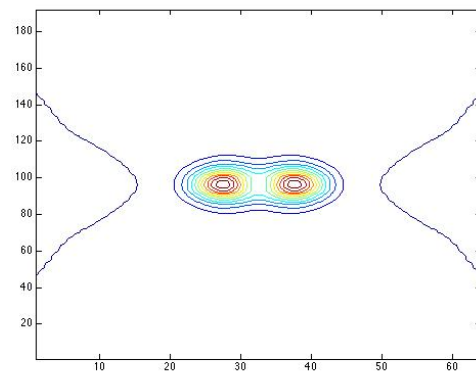
8.1 Original Rossby Soliton Solution



(a) Zonal Wind



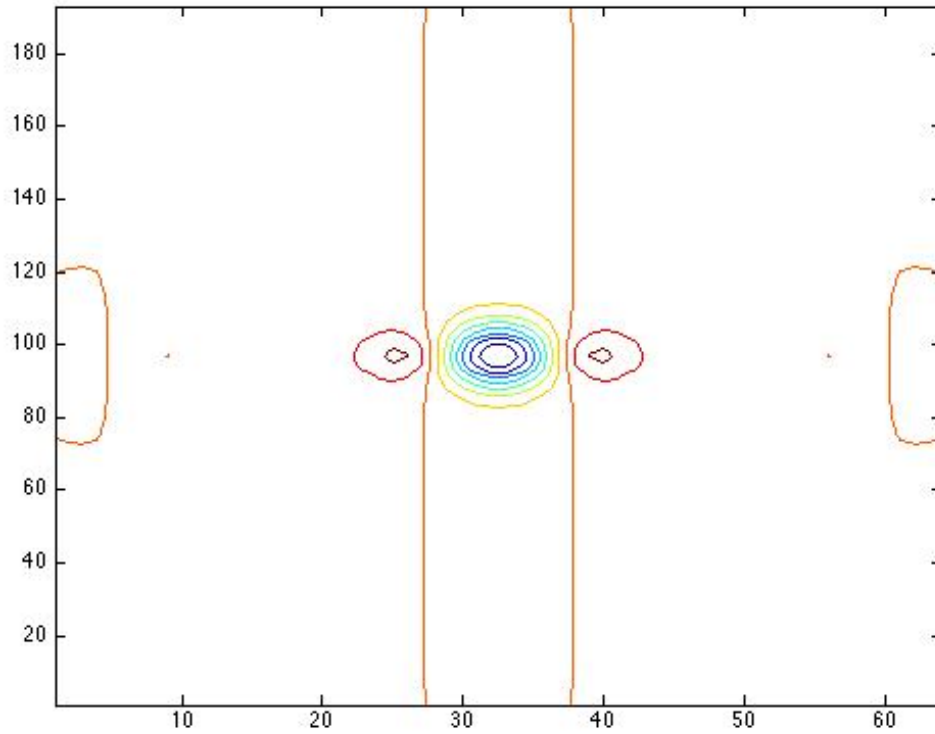
(b) Meridional Wind



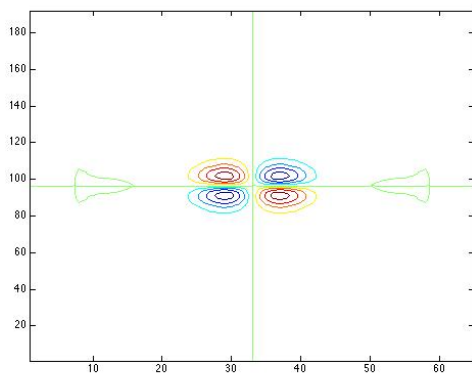
(c) Pressure

Figure 1: Original Rossby Soliton Solution

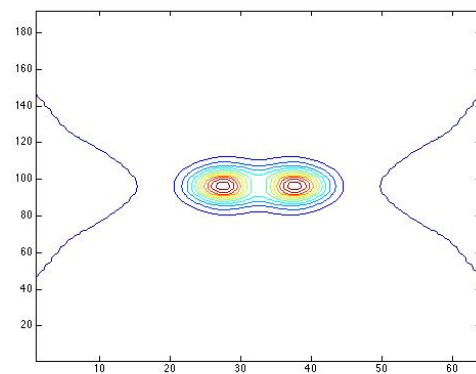
8.2 Edited Rossby Soliton Solution



(a) Zonal Wind



(b) Meridional Wind



(c) Pressure

8.3 Sea Level Pressure

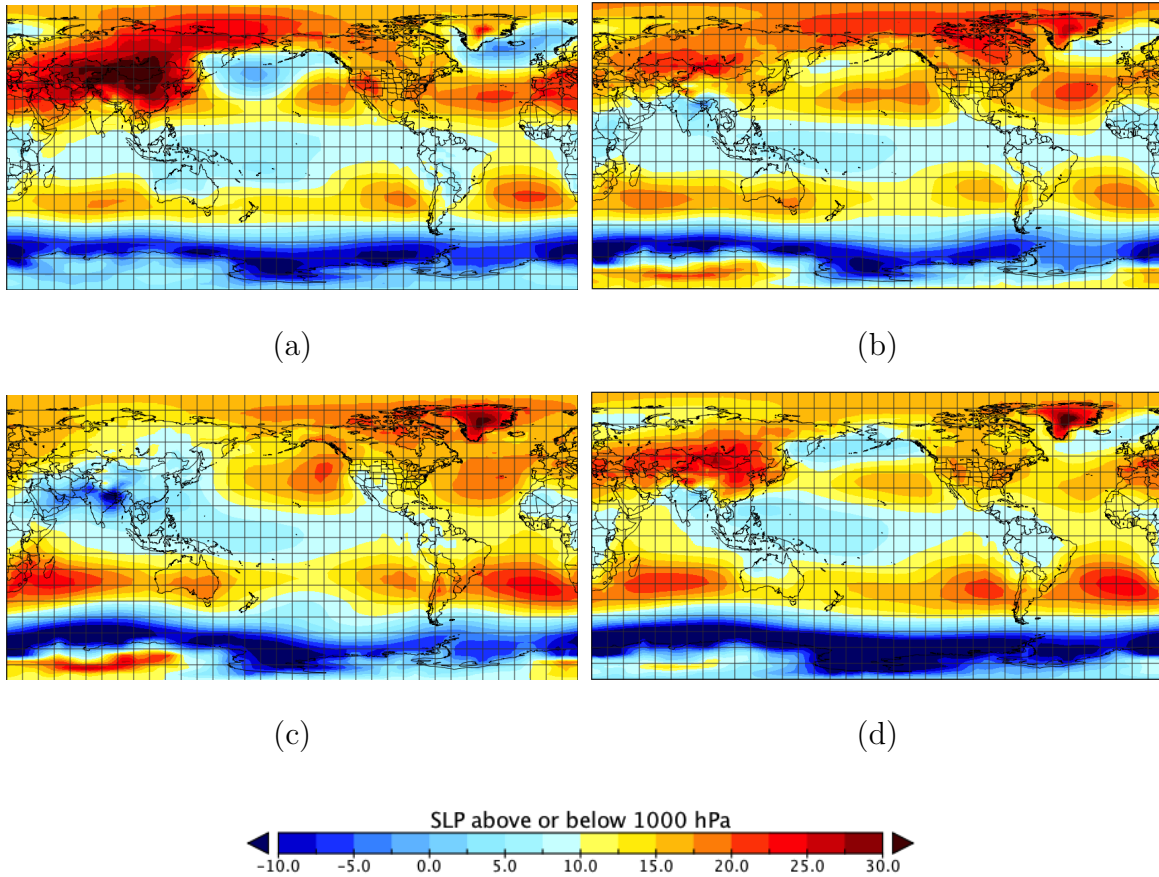


Figure 3: Average Sea Level Pressure averaged across each of the 4 seasons of the Validation Run, and for all 30 years. Red indicates the highest Sea Level Pressure, while blue indicates the lowest Sea Level Pressure. The North Pole is at the top of each figure while South is at the bottom. Winter is denoted by (a), Spring is (b), Summer is (c) and Autumn is (d).

8.4 Surface Wind Speed and Direction

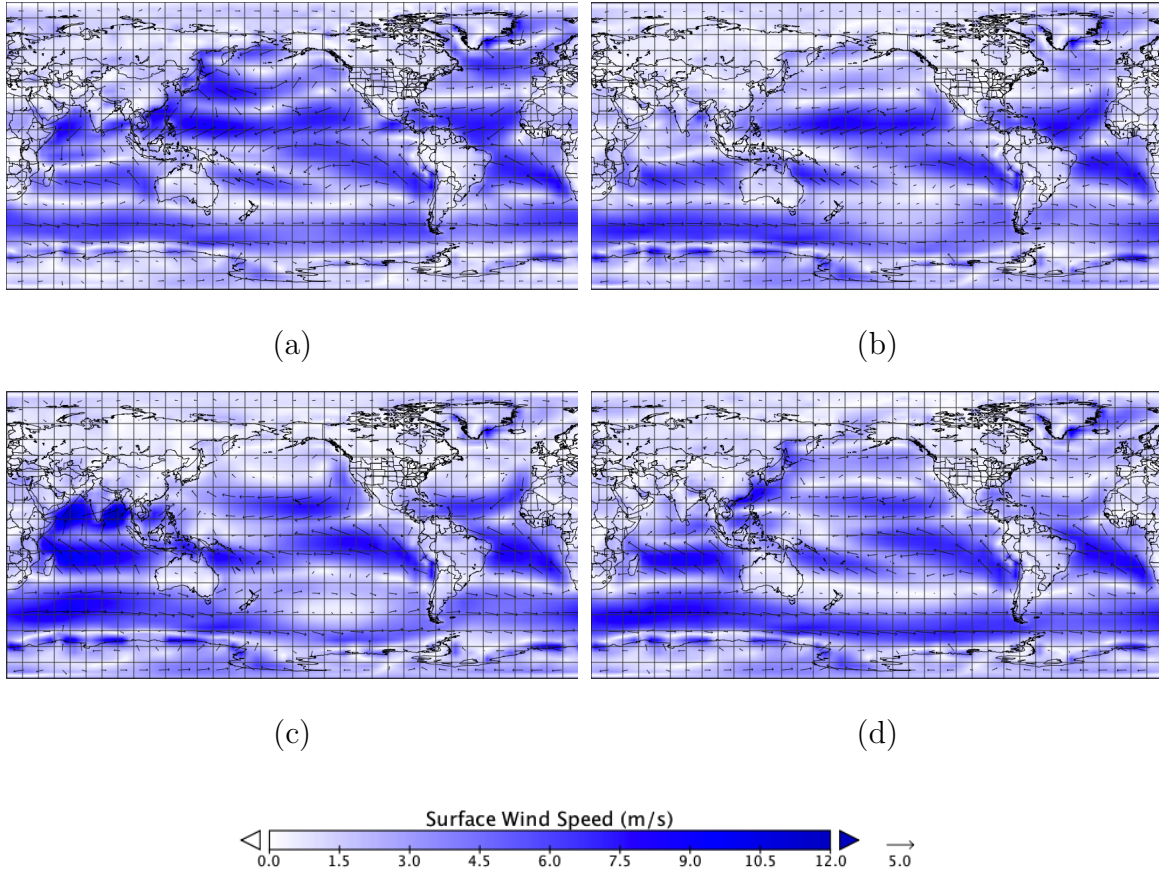


Figure 4: Average surface wind speeds and direction for each of the 4 seasons of the Validation Run, and for all 30 years. White are much weaker winds, with blue much stronger. Vectors indicate direction of the wind, and their size also indicates strength. Winter is denoted by (a), Spring is (b), Summer is (c) and Autumn is (d).

8.5 Zonal Wind

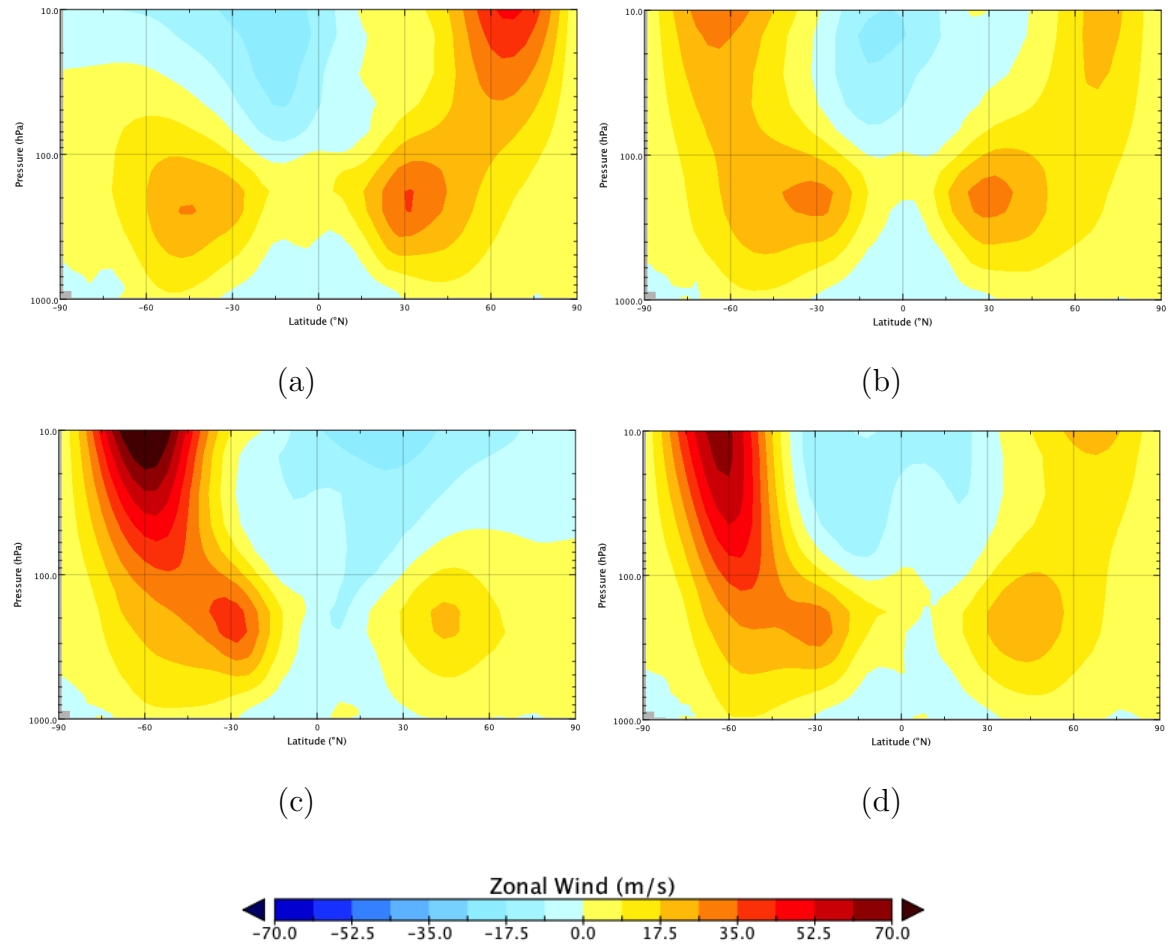


Figure 5: Zonal Winds averaged across each latitude and vertical pressure level from 1000 hPa to 10hPa, for each of the 4 seasons of the Validation Run, and for all 30 years. The North Pole is on the right of each figure and South is on the left. Positive values of wind are westerly winds and Negative values are easterly. Winter is denoted by (a), Spring is (b), Summer is (c) and Autumn is (d).

8.6 Atmospheric Temperature

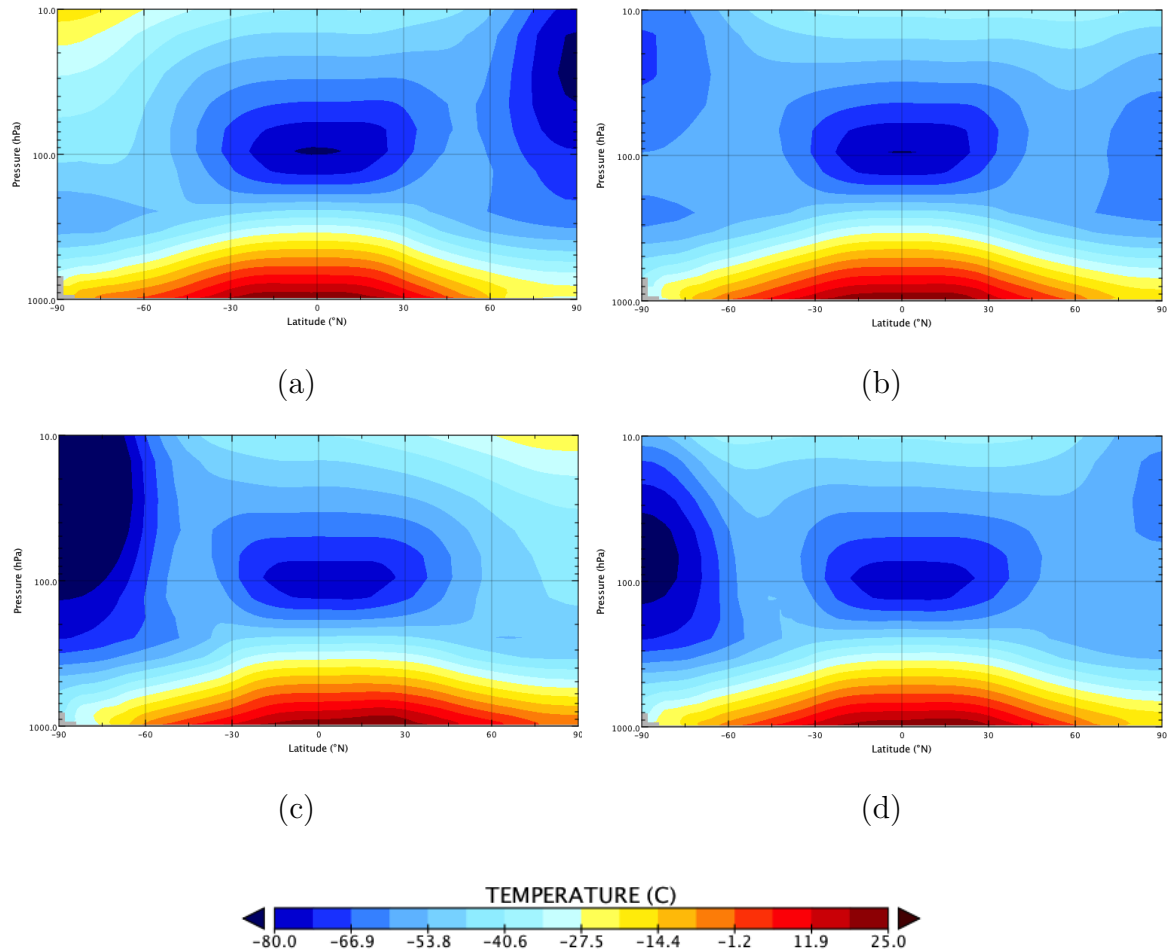


Figure 6: Atmospheric temperatures averaged across latitude and vertical pressure level from 1000hPa to 10hPa, for each of the 4 seasons of the Validation Run, and for all 30 years. Red indicates warmest temperatures, while blue indicates the coldest. North is on the right of each figure while South is on the left. Winter is denoted by (a), Spring is (b), Summer is (c) and Autumn is (d).

8.7 Sea Surface Temperature

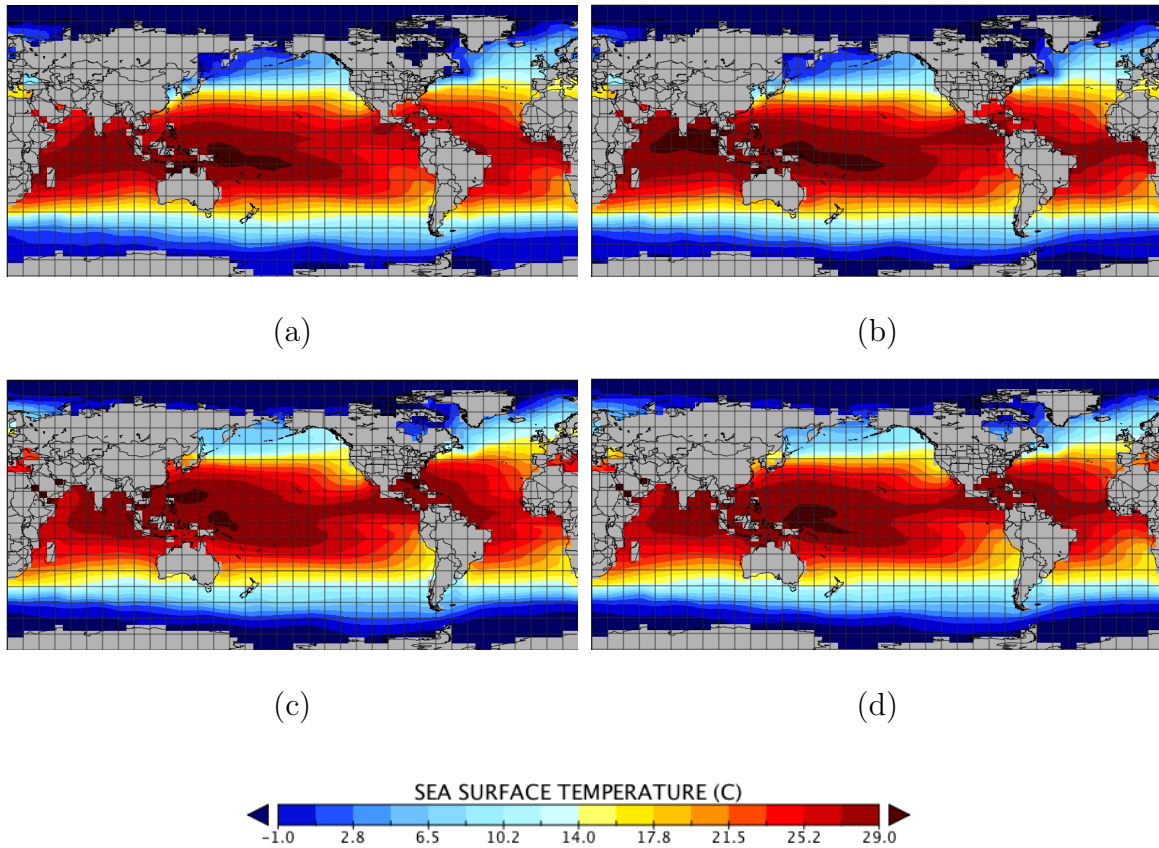


Figure 7: Average Sea Surface Temperature for each of the 4 seasons of the Validation Run, and for all 30 years. Red indicates the SST, while blue indicates the lowest SST. The North Pole is at the top of each figure while the South Pole is at the bottom. Winter is denoted by (a), Spring is (b), Summer is (c) and Autumn is (d).

8.8 Precipitation Patterns

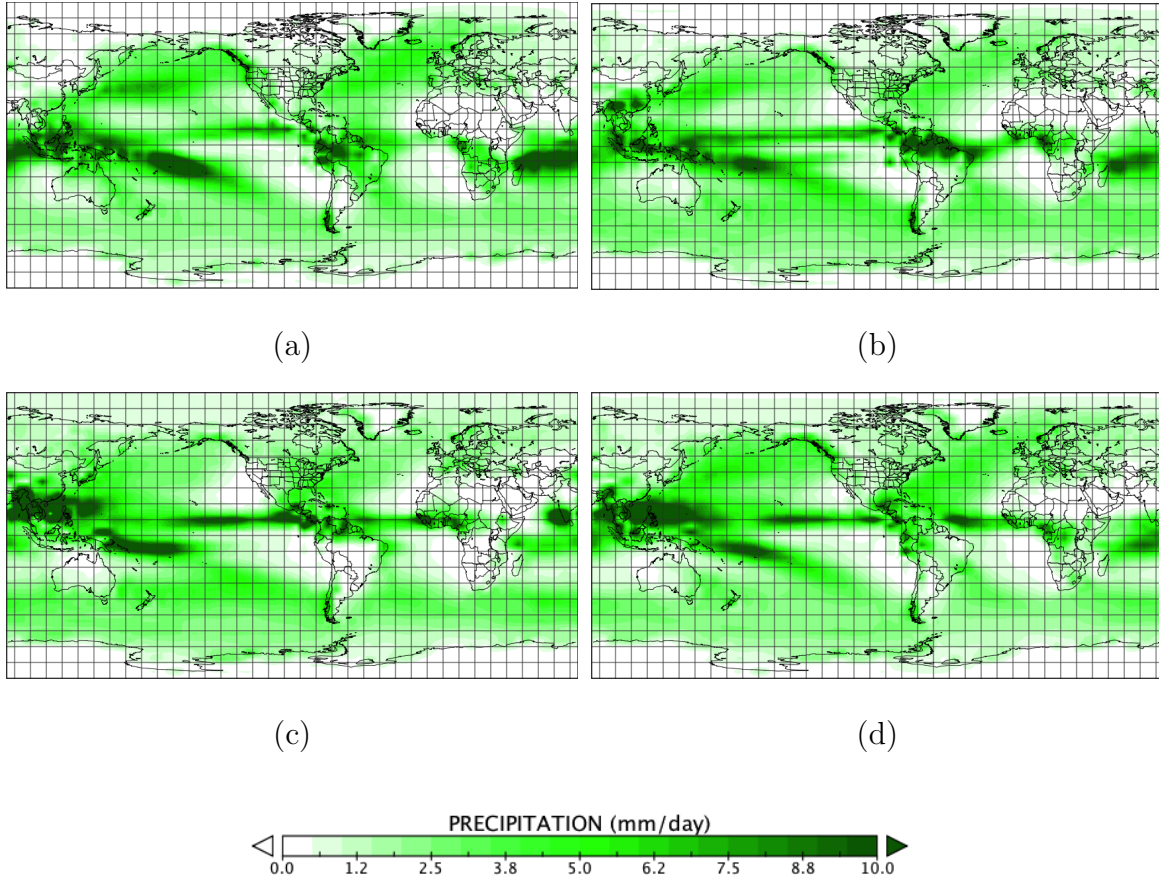


Figure 8: Average Precipitation averaged across each of the 4 seasons of the Validation Run, and for all 30 years. Green indicates the highest precipitation amounts, while white indicates the lowest. The North Pole is at the top of each figure while the South Pole is at the bottom. Winter is denoted by (a), Spring is (b), Summer is (c) and Autumn is (d).